Available online at www.sciencedirect.com

SciVerse ScienceDirect

Ceramics International 38 (2012) 6389–6397

CERAMICS INTERNATIONAL

www.elsevier.com/locate/ceramint

Influence of cooling mode on the electrical properties and microstructure of $Ba_{1.022-x}Sm_xTiO_3$ ceramics sintered in a reducing atmosphere

Dongxiang Zhou, Xuxin Cheng, Qiuyun Fu*, Shuping Gong, Dongchen Zhao

Engineering Research Center for Functional Ceramics MOE, Department of Electronic Science and Technology, Huazhong University of Science and Technology, Luoyu Road 1037, Hongshan District, Wuhan 430074, Hubei, PR China

Received 2 February 2012; received in revised form 26 April 2012; accepted 4 May 2012
Available online 17 May 2012

Abstract

We investigated the effects of the Sm-dopant content and the cooling rate on the electrical properties and microstructure of $Ba_{1.022-x}Sm_xTiO_3$ (BST) ceramics, which were sintered at 1200 °C for 30 min in a reducing atmosphere and then reoxidized at 800 °C for 1 h. The results indicated that the cooling rate affected the electrical properties and the microstructure of the BST samples, whose room-temperature resistivity increased with increasing cooling rate. The semiconducting BST ceramics showed a pronounced positive temperature coefficient of resistivity effect, with a resistance jump greater by 3.16 orders of magnitude, along with a low room-temperature resistivity of 157.4 Ω cm at a cooling rate of 4 °C/min. The room-temperature resistivity of the specimen was lower after sintering for 30 min at 1150 °C during cooling.
© 2012 Elsevier Ltd and Techna Group S.r.l. All rights reserved.

Keywords: Cooling rate; $BaTiO_3$; PTCR effect; Sm_2O_3-dopant

1. Introduction

Barium titanate ($BaTiO_3$) is a ferroelectric material, which transforms from a tetragonal perovskite structure (ABO_3) at room temperature into a cubic (paraelectric) structure at the Curie temperature, $T_c \sim 130$ °C [1]. Undoped $BaTiO_3$ is an electrically insulating material; however, if the ions at the A or B site of $BaTiO_3$ are substituted by (doped with) small quantities of a trivalent donor (such as Y^{3+}, Sm^{3+}, La^{3+}, Sb^{3+}, etc.) or pentavalent impurities (such as Nb^{5+}, Ta^{5+}, etc.), $BaTiO_3$ becomes a semiconducting material and shows an anomalous increase in resistivity at temperatures close to the T_c [2,3]. The phenomenon is commonly known as the positive temperature coefficient of resistivity (PTCR) effect. The most widely accepted explanation for this effect has been proposed by Heywang [4] and later modified by Jonker [5]. The PTCR effect of doped $BaTiO_3$ ceramics is regarded as a grain-boundary characteristic.

Donor-doped $BaTiO_3$ ceramics show much higher room-temperature resistivity and jumping ratios when they are sintered in air than when sintered in a reducing atmosphere; however, low room-temperature resistivity of PTCR ceramics has been obtained by a reduction–reoxidation method [6–8]. Moreover, to further decrease the resistivity, specimens with a multilayer structure can be produced [9–11]. Meanwhile, for preventing the oxidation of the inner Ni electrodes, the green samples are cofired in a reducing atmosphere. Therefore, investigating the cooling method in a reducing atmosphere is important. Recent experiments by Chung [12] have suggested that the room-temperature resistivity is affected by the sintering temperature. Lee et al. [13] claim that the PTCR effect and the room-temperature resistivity of ceramics increase with decrease of the cooling rate in air. Lowering the cooling rate after sintering in air increases the resistivity jump, decreases the room-temperature resistivity [14–18], and does not alter the microstructure [14,15]. The bulk resistivity is affected only slightly by increases in the cooling rate. A reduction in room-temperature resistivity with increasing cooling rate is consistent with a reduction in the ratio of

*Corresponding author. Tel./fax: +86 27 8754 5167.
E-mail address: fuqy@mail.hust.edu.cn (Q. Fu).

0272-8842/$36.00 © 2012 Elsevier Ltd and Techna Group S.r.l. All rights reserved.
http://dx.doi.org/10.1016/j.ceramint.2012.05.011

unit residual surface charge density to permittivity and activation of surface state density [15,17]. Yoon et al. [19] propose that donor segregation could occur during the cooling process that follows heat treatment in air.

However, little attention has been paid to the change in the cooling mode during the cooling period and its effect on both the PTCR characteristics and the microstructure of the particles produced in a reducing atmosphere. Previous studies have focused only on oxidation at grain boundaries during the cooling period in air. Furthermore, the cooling mode appears to change both the microstructure of the particles and the solidification characteristics. Therefore, the objective of this study is to investigate the effects of (1) the cooling rate and (2) the cooling mode on the microstructure and the PTCR characteristics of $Ba_{1.022-x}Sm_xTiO_3$ ceramics produced in a reducing atmosphere.

2. Experimental procedures

The starting materials were high-purity $BaCO_3$, TiO_2, SiO_2, and Sm_2O_3, and they were weighed according to the following formula: $(Ba_{1.022-x}Sm_x)TiO_3 + 0.007$ mol SiO_2. In this experiment, the Ba-site/Ti-site ratio was maintained at 1.022. The components were mixed by wet ball milling for 4 h in deionized water using zirconia balls in a polyurethane jar and then calcined at 1150 °C for 2 h in air. After drying and sieving, the calcined powder was ground again by ball milling for 4 h. After mixing, the dried powder was mixed with dispersant, defoamer, solvent, and binder by ball milling for 18 h in a nylon pot and cast into green sheets of 55-μm thickness by the doctor-blade method. These sheets were stacked and laminated at 50 °C to form a ceramic block, which was cut into rectangular blocks ($5.7 \times 3.9 \times 1$ mm). Subsequently, the binder was removed by heating at 280 °C in air. Sintering was conducted in an aluminum tube at 1200 °C for 30 min in a reducing atmosphere (3% H_2/N_2), with the heating and cooling rates being 5 and 3 °C/min, respectively, at a flow rate of 200 cm^3/min under a pressure of 1 atm. The bulk densities and porosities of the sintered specimens were measured using the Archimedes method. Four different cooling curves were used for our present experiment, as shown in Table 2. The sintered BST ceramics were reoxidized at 800 °C in air for one hour, and the surfaces were rubbed with In–Ga alloy (60:40) to form electrodes. Resistance at room temperature was measured by a digital multimeter, and the temperature dependence of resistance was measured in a temperature-programmable furnace at a heating rate of 1.6 °C/min in the range 25–250 °C. An inductance (L), capacitance (C), and resistance (R; LCR) digital bridge was used to measure the fixed-frequency capacitance during the process of heating from room temperature to 250 °C at a heating rate of 2 °C/min, with the data being recorded at a frequency of 10 kHz. The surface microstructure of the as-sintered ceramics was observed using field-emission scanning electron microscopy (FESEM; Sirion 200, FEI Corp., the Netherlands); energy-dispersive X-ray spectrometry (EDAX) was used to obtain the morphology and chemical composition of individual grains and the grain boundaries. The average grain size of the BST ceramics was estimated by the line-intersection method. Complex impedance spectroscopy over the range 100 Hz–35 MHz was measured using an impedance analyzer (HP4294A, Agilent, USA).

3. Results and discussion

3.1. Microstructure of the ceramics

The microstructure of the samples is significantly affected by the cooling rate (Fig. 1), and a noticeable difference in the grain size is observed. The average grain sizes of the samples shown in Fig. 1(a–e) are 1.59, 1.44, 1.43, 1.40 and 1.32 μm, respectively; moreover, it decreases and becomes uniform with increase in cooling rate, probably due to the slight increase in the porosity with an increase in the cooling rate. Therefore, the particle-size distribution may be due to differences in the rates of grain growth. The liquid phase can be solidified by cooling from 1200 to 800 °C, and both the movement of the grain boundary and the mass-transfer process become slower due to an increase in the cooling rate. The particle-size distribution on the surfaces of the as-sintered specimens sintered at 1200 °C and subjected to different cooling rates is shown in Fig. 2. From Fig. 2c, the particle-size distribution of the sample is observed to be in accordance with a normal distribution.

3.2. Influence of the cooling rate on electrical properties

The dependence of the room-temperature resistivity of the semiconducting BST ceramics, reoxidized at 800 °C for one hour after sintering at 1200 °C for 30 min in a reducing atmosphere, on the dopant concentration is shown in Fig. 3. From the figure, the room-temperature resistivity can be found to decrease with increase in the content of doped Sm for samples subjected to a low cooling rate (< 3 °C/min); however, it first reduces and then increases as a function of the dopant concentration at a high cooling rate (≥ 3 °C/min). This phenomenon signifies that the lesser the cooling rate, the smaller is the resistivity. Furthermore, the corresponding dopant concentration of the minimum resistivity is shifted to lower values with increasing cooling rate. The decrease in resistivity is generally attributed not only to the electron compensation of the substituted Ba^{2+} by the Sm^{3+} [20], but also to the formation of the following oxygen vacancies:

$$Sm_2O_3 \rightarrow 2Sm_{Ba}^{\bullet} + 2O_0 + 1/2O_2 + 2e' \quad (1)$$

$$O_0 \rightarrow V_0^{\bullet\bullet} + 1/2O_2 + 2e' \quad (2)$$

The increase in resistivity is due to the ionic compensation resulting from the formation of cation and oxygen vacancies. However, the critical concentration of the cation vacancies can be greatly suppressed by the oxygen vacancies, and it is increasingly higher at higher cooling rates.

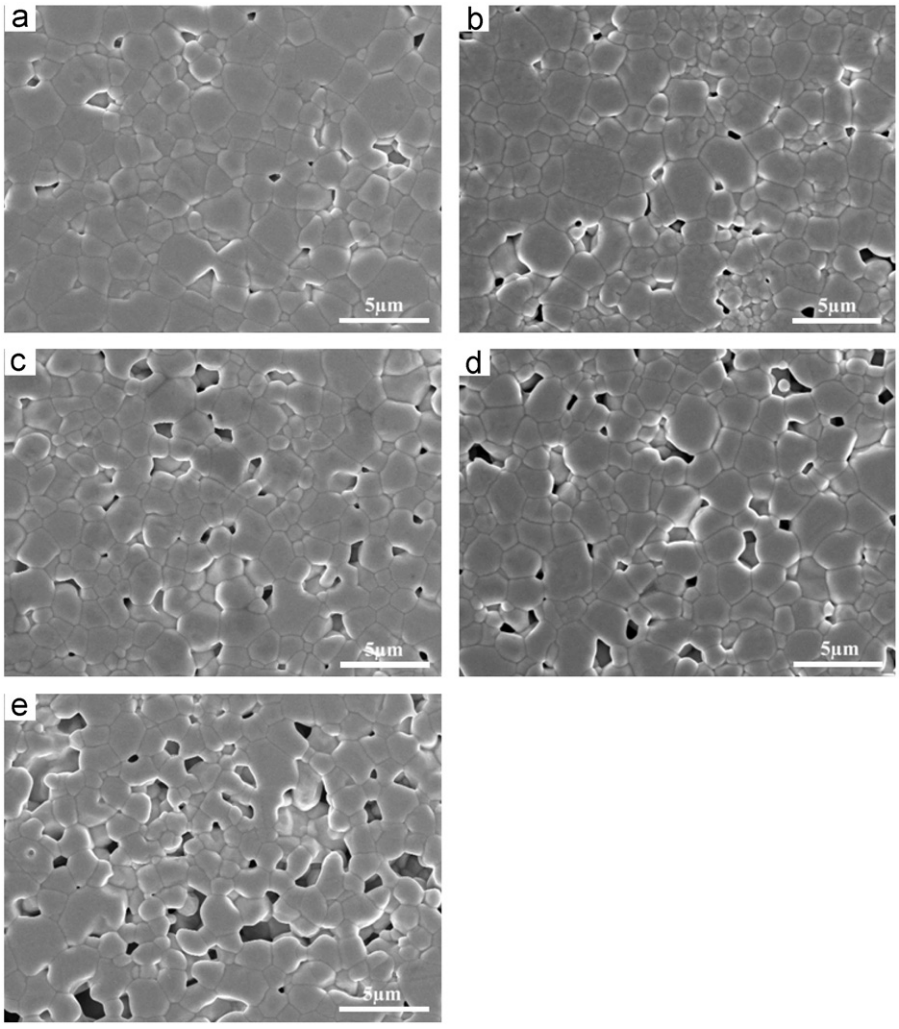

Fig. 1. The SEM micrograph on the surfaces of the as-sintered specimens sintered at 1200 °C with different cooling rates; (a) 2, (b) 3, (c) 4, (d) 5 and (e) 7 °C/min.

Thus, the concentration of the cation vacancies plays a dominant role. Moreover, the critical concentration of the dopant closely depends on the cooling rate.

3.3. Influence of the cooling rate on PTCR effect

The room-temperature resistivity and the jumping ratio ($Lg(R_{max}/R_{min})$) of the 0.40 mol% Sm-doped $BaTiO_3$ ceramics are shown in Fig. 4 as functions of the cooling rate, and the influence of the cooling rate on the PTCR characteristics is shown in Fig. 5. The room-temperature resistivity of the samples that are reoxidized at 800 °C for 1 h after sintering at 1200 °C for 30 min increases with an increase in the cooling rate from 2 to 7 °C/min. The corresponding jumping ratio also increases with the increase in the cooling rate from 2 to 4 °C/min; subsequently, it slightly decreases with increasing cooling rate across the range of 4–7 °C/min. The highest resistance-jumping ratio is obtained at the cooling rate of 4 °C/min, which is exhibited by 3.16 orders of magnitude, with the room-temperature resistivity being 157.4 Ω cm.

The densities (ρ) of ceramic specimens obtained at different cooling rates are distinct. The relative densities (D) of the ceramics are shown in Fig. 6: the samples obtained under a cooling rate of 2 °C/min have much higher densities than those obtained at 4 °C/min; the samples obtained at a cooling rate of 7 °C/min have the lowest density. In addition, the characteristics of the porosity for P, P_0 and P_1 which are the apparent porosity, true porosity and closed porosity, respectively, which are shown in Table 3, it is indicated that the apparent porosity of the samples of 2 and 7 °C/min are 0.95% and 9.57%, respectively. According to Kuwabara [21], in the case of PTCR ceramics, the magnitude of the PTCR effect decreases with an increase in their densities due to the porous nature of the ceramics having lower densities. Thus, higher densities of the samples may reduce the PTCR effect because absorption of oxygen during the process of reoxidation becomes difficult. On the basis of their porosities of the samples obtained at high cooling rates in comparison with those obtained at a low cooling rate, we can infer that the porosity play an important role

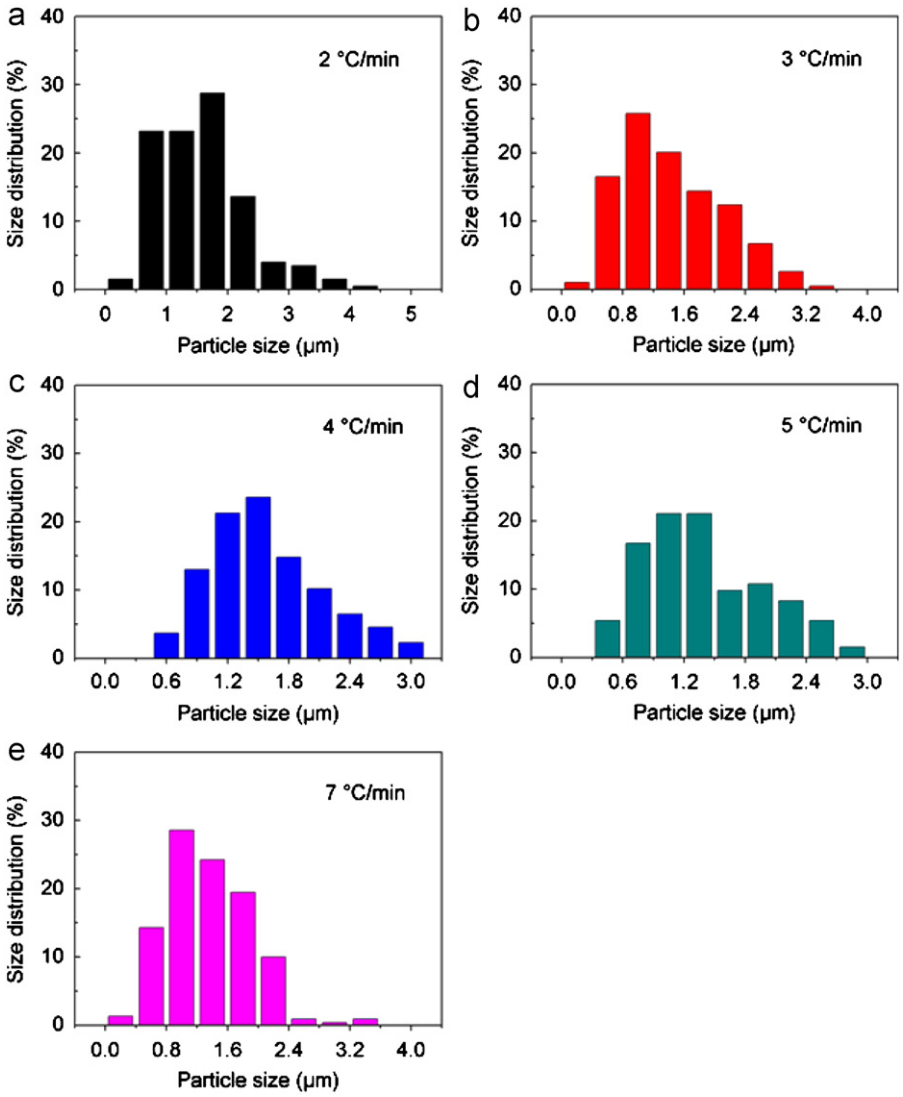

Fig. 2. The particle-size distribution on the surfaces of the as-sintered specimens sintered at 1200 °C with different cooling rates; (a) 2, (b) 3, (c) 4, (d) 5 and (e) 7 °C/min.

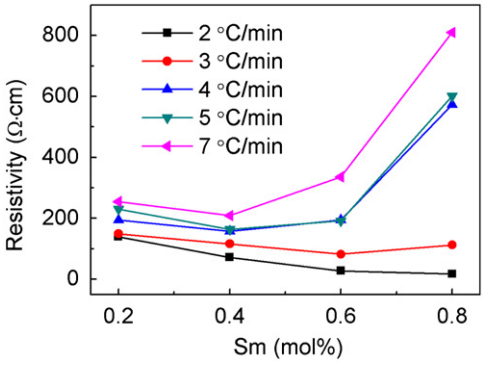

Fig. 3. The room-temperature resistivity is as a function of the dopant concentration at different cooling rates.

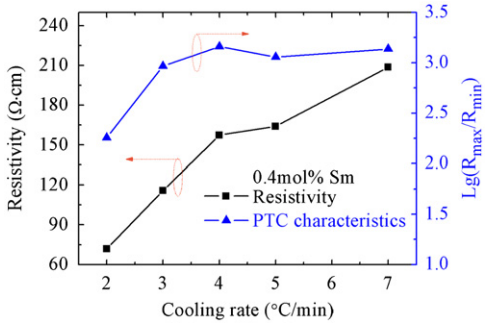

Fig. 4. The room-temperature resistivity and the jumping ratio are as a function of the cooling rate.

in the PTCR effect. Therefore, the specimens obtained at high cooling rates show pronounced PTCR characteristics.

Alternatively, BST ceramics obtained at a lower cooling rate show modest room-temperature resistivity and PTCR characteristics, which indicates that some oxygen anion vacancies of the $BaTiO_3$ perovskite lattice cannot be completely filled up by the oxygen atoms present in air. This is because the diffusion and permeation of oxygen

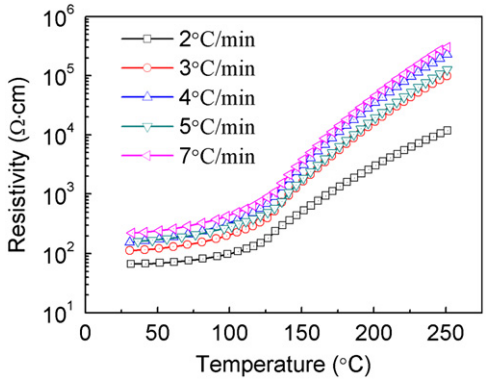

Fig. 5. The temperature dependence of resistivity for different cooling rates.

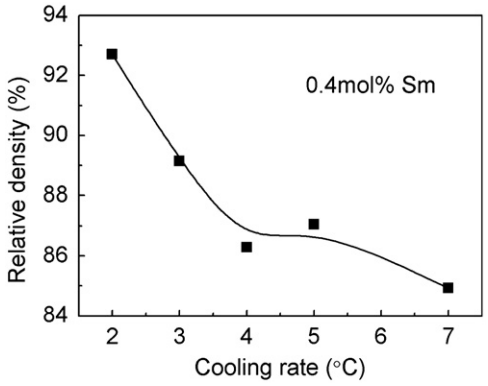

Fig. 6. The relative densities of the ceramics are as a function of the cooling rate.

atoms from the air into compact ceramics becomes difficult. According to the following expression, $V_0^{\bullet\bullet}+1/2O_2+2e' \rightarrow O_0$, the localized electrons and oxygen vacancies around the defects are annihilated; therefore, the room-temperature resistivity of the ceramics obtained at a low cooling rate is reduced.

3.4. FESEM–EDAX analyses

FESEM–EDAX analyses are used to obtain detailed information regarding the three intergranular phases. From the results of semiquantitative EDAX, only Ba, Ti, O, and C are found in the matrix, as shown in Fig. 7b and d, Fig. 8b and d. It indicates that a greater number of barium and titanium ions are present in the grain-boundary area (*B*) than at the center of the grain (*A*). Furthermore, from the FESEM micrographs of the surfaces of the polished samples (Fig. 1a and e), a slower cooling rate (2 °C/min) can result in a larger amount of the second phase in the grain-boundary area [16]. This second phase is expected to be barium orthotitanate, Ba_2TiO_4 [22,23]. In addition, a larger amount of oxygen is found in the midgrain region than at the grain boundary with the use of a higher cooling rate (7 °C/min). This indicates that a higher cooling rate leads to a larger number of oxygen losses in the grain-boundary region, because the cooling rate has been found to change the defect chemistry near the grain boundaries [14,16,18]. Thus, to improve the PTCR characteristics, the reoxidation process is widely

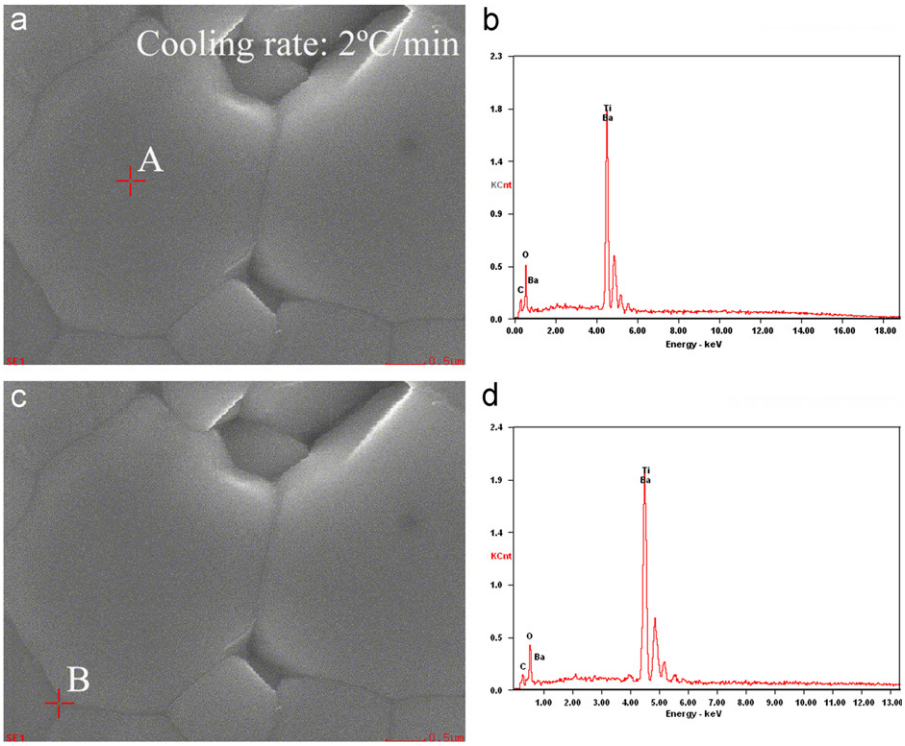

Fig. 7. FESEM–EDAX images of the ceramics under a cooling rate of 2 °C/min.

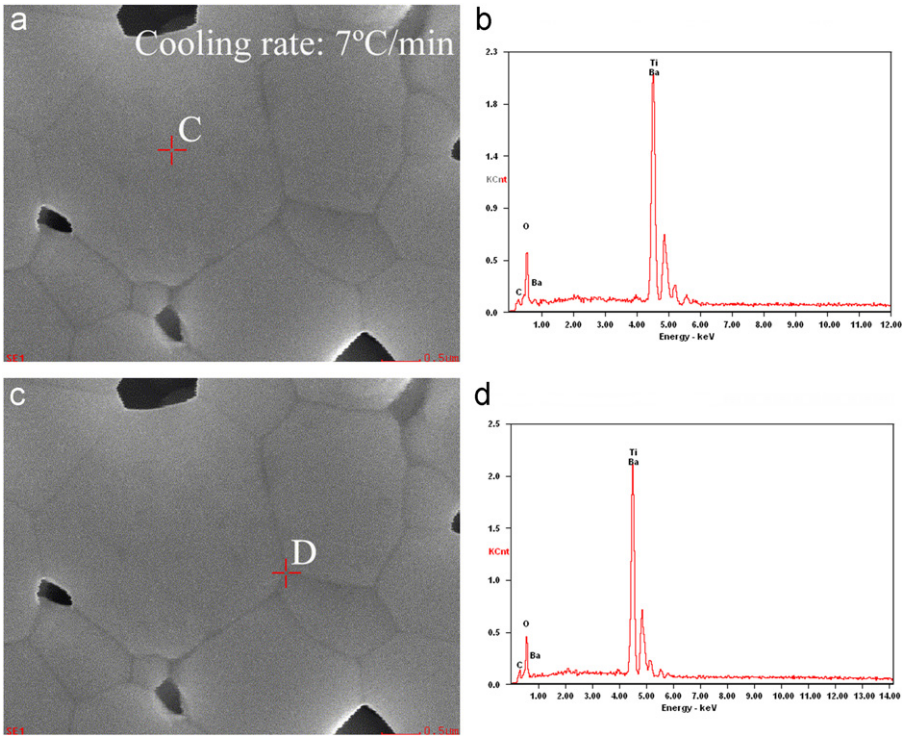

Fig. 8. FESEM–EDAX images of the ceramics under a cooling rate of 7 °C/min.

Table 1
The content of the chemistry elements for different points.

Point	Elements			
	BaL (at%)	TiK (at%)	OK (at%)	CK (at%)
A	13.66	17.71	37.53	31.11
B	16.89	22.42	37.19	23.50
C	16.87	20.73	47.29	15.11
D	16.55	22.25	42.41	18.79

carried out in air. Furthermore, region *D* indicates that a higher content of grain-boundary phase exists at triangular junctions and that a higher cooling rate is accompanied by an increase in the amounts of the grain-boundary phase [13]. In addition, according to the Heywang and Jonker models explaining the resistance anomaly and Eq. (2), the outward diffusion of oxygen vacancies [18], after leaving the free electron behind, is proposed to cause the formation of both the defect complex and the "$V_0^{\bullet\bullet}-2e'$" pair. The phenomenon by which a lower cooling rate reduces the room-temperature resistivity of specimens is attributed to the higher concentration of free electrons in the samples. Consequently, differences in the cooling rate can be assumed to have an effect on the formation of the defect complex. Slower cooling rates help the formation of the defect complex by the charge-balance path, because they provide more time for the oxygen vacancies to diffuse from the matrix grains to the grain boundaries. Therefore, the decrease in *O* content of the matrix grains with decrease in the cooling rate, as shown in Table 1, provides the evidence for this assumption about the defect complex.

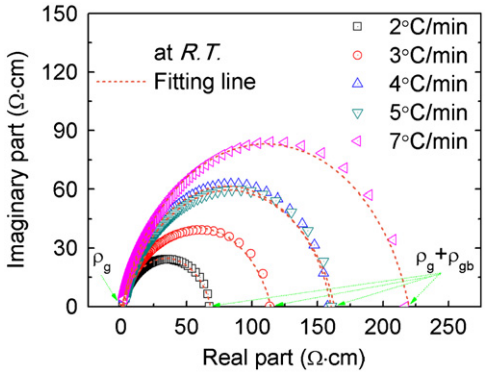

Fig. 9. The complex-plane impedance diagrams of the specimens with different cooling rates.

3.5. Impedance analysis

The complex-plane impedance diagrams of the specimens in Fig. 4 are presented in Fig. 9. Both grain resistivity and grain-boundary resistivity are calculated from Fig. 9 by a semicircle-fitting method; moreover, the experimental data are in good agreement with the fitting line. The results in Fig. 10 show that the grain resistivity of the samples is nearly unaffected by the cooling rate; however, the grain-boundary resistivity increases with increase in the cooling rate and is the highest at the cooling rate of 7 °C/min.

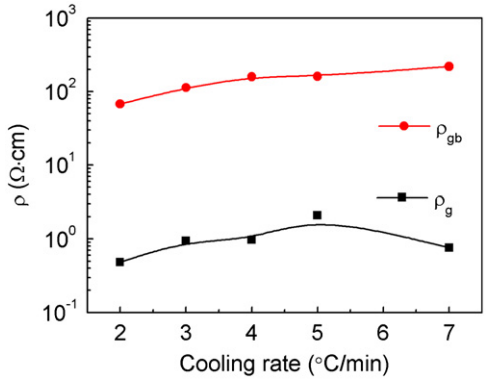

Fig. 10. The room-temperature resistivity of the samples with the grains and grain boundaries is as a function of the cooling rate.

From this result, the PTCR effect in the samples obtained at the cooling rates of 4–7 °C/min is considered to be enhanced because the easier reoxidation of the grain boundary results in the increase in grain-boundary resistivity [24] compared to the specimens obtained at a cooling rate of 2 °C/min. Furthermore, a porous structure [25] is observed on the surface of the former as-sintered samples, which is favorable for the reoxidation of the grain boundary and the subsequent formation of Schottky barriers. Thus, we can conclude that the room-temperature resistivity of grain boundaries of the samples is affected by the cooling rate. In addition, according to the semiconductor theory of the resistivity [3,4], it can be inferred that the height of the Schottky barrier (ϕ) increases also with the increasing cooling rate because it is basically in proportion to the room-temperature resistivity of the grain boundaries.

3.6. Acceptor-state density (N_s) and height of the potential barrier (ϕ)

According to the Heywang–Jonker model [3–5], when the temperature of the sample is below the T_C, the potential barrier is neutralized by the electric barriers formed by ferroelectric polarization. At temperatures above the T_C, however, the height of the potential barrier (ϕ) is given by the expression

$$\phi(T > T_C) = eN_S^2/8\varepsilon_0\varepsilon_r N_d \quad (3)$$

and ε_r is given by the Curie–Weiss law, as follows:

$$\varepsilon_r = C/(T-\theta) \quad (4)$$

where N_s is the acceptor-state density, N_d is the donor concentration, e is the electric charge, ε_r is the relative permittivity of the $BaTiO_3$ ceramics, ε_0 is the vacuum permittivity, C is the Curie constant ($\sim 1.5\times10^5$ K) [16,22,26,27], T is the absolute temperature, and θ corresponds to the Curie–Weiss temperature [1,2]. According to the semiconductor theory, the grain-boundary resistivity is given by the following formula:

$$\rho = \rho_0 \exp(e\phi/\kappa_B T) \quad (5)$$

where κ_B is the Boltzmann constant and ρ_0 is a constant. Therefore, from Eqs. (3) and (5), ρ can be represented as

$$\rho = \rho_0 \exp(e^2 N_S^2/8\varepsilon_0\varepsilon_r N_d \kappa_B T) \quad (6)$$

The $\varepsilon'(T)$ is given by $\varepsilon'(T) = \varepsilon_r \cdot r/2b$ [28,29], where $\varepsilon'(T)$ is the apparent dielectric constant, r is the average grain size, b ($= N_s/2N_d$) is the depletion layer thickness of the Schottky barrier, in Eq. (6), ρ can be rewritten as

$$\rho = \rho_0 \exp(e^2 N_S r/8\varepsilon_0\varepsilon'(T)\kappa_B T) \quad (7)$$

According to Eq. (7), the Arrhenius plots of lnρ against $1/[T\cdot\varepsilon'(T)]$ are shown in Fig. 11, where the resistivity data (ρ) is measured every 5 °C above T_C from the resistivity–temperature curves in Fig. 5 and the apparent dielectric constant [$\varepsilon'(T)$] is calculated from the measured capacitance, as follows: $\varepsilon'(T) = C_p t/\varepsilon_0 A$, where C_p is the capacitance of a sample, t is the thickness of a sample, A is the electrode area of the surface for a sample. The experimental points lie on a straight line within the temperature range between the T_C and T_{max}. The slope λ of the Arrhenius plots is given by the expression

$$\lambda = e^2 N_s r/8\varepsilon_0\kappa_B = BN_s. \quad (8)$$

The value of N_s, as calculated from Eq. (8) for the samples, is in the range from 7.54×10^{13} to 3.40×10^{14} cm^{-2}. As shown in Fig. 12, a higher cooling rate leads to lower values of N_s, which decreases with a decrease in the amounts

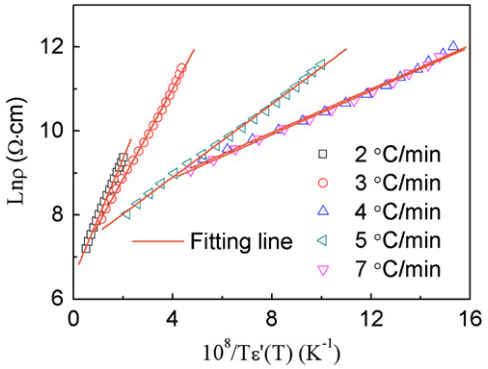

Fig. 11. The Arrhenius plots of lnρ against $1/T\varepsilon'(T)$ for the BST ceramics which are sintered at 1200 °C for 30 min. and cooled by various rates in a reducing atmosphere.

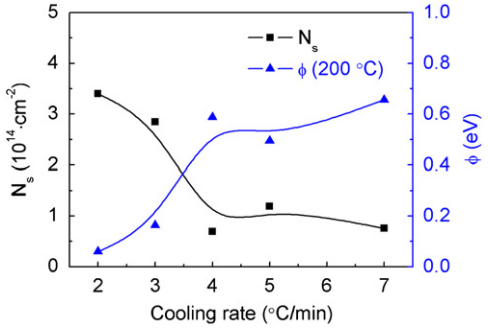

Fig. 12. The acceptor-state density and height of the potential barrier are as a function of the cooling rate.

of oxygen atoms absorbed at the grain boundaries [5]. From Eqs. (5) and (7), we have $\phi = eN_s r/8\varepsilon_0\varepsilon'(T)$. As shown in Fig. 12, the height of the potential barrier also increases with the cooling rate; therefore, from Eq. (5), the room-temperature resistivity values of the specimens increase with the cooling rate, and the potential-barrier heights of the samples obtained at the cooling rates of 2 and 7 °C/min are 0.06 and 0.66 eV, respectively.

3.7. Influence of the cooling duration on PTCR effect

The temperature dependence of resistivity of the 0.4 mol% Sm-doped BST ceramics for various cooling curves is as shown in Fig. 13. The samples are cooled at different cooling modes after sintering at 1200 °C for 30 min and then reoxidized at 800 °C for 1 h. The cooling curves and their corresponding times are shown in Table 2. On comparing the experimental results, the room-temperature resistivity of the C1 ceramics is found to be less than that of both C2 and C3 ceramics, showing a significant PTCR effect with a resistance-jumping ratio of 3.0, 3.2, and 3.3, respectively. However, the room-temperature resistivity of the C4 specimens obtained by furnace cooling is quite high. This is because the concentration of oxygen vacancies in the C4 samples is higher than that in the others in the grain-boundary region, with a correspondingly low relative density. Thus, the oxygen vacancies can be adequately compensated by the oxygen atoms from air, and the grain boundaries are oxidized. This can lead to an increase in the acceptor states, thus resulting in

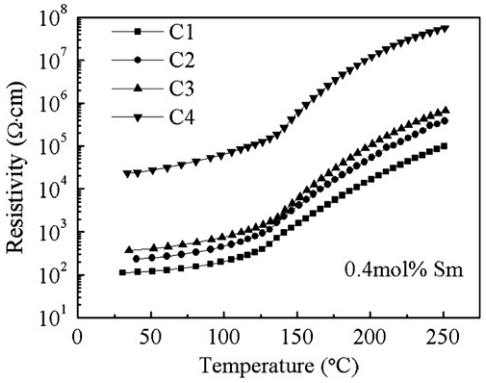

Fig. 13. The temperature dependence of resistivity for different cooling curves.

Table 2
The various cooling curves during cooling.

The temperature range (°C)	Samples and the cooling time (min)			
	C1	C2	C3	C4
1200→1150	17	17	17	FC[a]
1150→1150	30	0	30	FC
1150→800	117	117	FC	FC
800→Rt.	FC	FC	FC	FC

[a]Furnace cooling.

Table 3
The characteristics of the porosity for the 0.4 mol% Sm-doped BST ceramics versus the different cooling rates.

Cooling rate (°C/min)	Characteristics of the porosity				
	ρ (g/cm^3)	D (%)	P (%)	P_0 (%)	P_1 (%)
2	5.58	92.70	0.95	7.30	6.35
3	5.37	89.14	5.50	10.86	5.35
4	5.19	86.28	7.96	13.72	5.75
5	5.24	87.05	7.14	12.95	5.80
7	5.11	84.93	9.57	15.07	5.51

a larger room-temperature resistivity. This result indicates that the electrical properties of the ceramics are closely related to the cooling rates. From Fig. 13, the lowest room-temperature resistivity is found in the samples cooled from 1200 to 800 °C at a cooling rate of 3 °C/min and sintered at 1150 °C for 30 min during cooling. The results show that the room-temperature resistivity can be reduced by prolonging the cooling duration because the concentration of free electrons increases significantly after prolongation of the cooling duration, as seen in Eq. (2), resulting in a decrease in the room-temperature resistivity of the samples. Table 3

4. Conclusions

The influence of the cooling method on the electrical properties and microstructure of BST-based ceramics sintered at 1200 °C for 30 min in a reducing atmosphere and reoxidized at 800 °C for one hour in air has been herein investigated. The results show that the room-temperature resistivity of the BST ceramics increases with increase in the cooling rate, and lower room-temperature resistivity is obtained by prolonging the cooling duration. The critical concentration of the dopant closely depends on the cooling rate. Meanwhile, the grain size of the specimen slightly decreases with increase in the cooling rate. In addition, samples that have been cooled at a cooling rate of 4 °C/min after sintering in a reducing atmosphere show pronounced PTCR characteristics, with a resistance-jumping ratio greater by 3.16 orders of magnitude, in addition to achieving a low room-temperature resisitivity of 157.4 Ω cm. Furthermore, the acceptor-state density (N_s) and height of the potential barrier (ϕ) for these samples are 6.91×10^{13} cm^{-2} and 0.59 eV, respectively.

Acknowledgments

This work was financially supported by the Ministry of Science and Technology of China through 863 Program (no. 2009AA03Z445). We would like to express our appreciation to Ms. Xianhui Gao for the FESEM measurement.

References

[1] M.W. Mancini, P.I. Paulin Filho, Direct observation of potential barriers in semiconducting barium titanate by electric force microscopy, Journal of Applied Physics 100 (2006) 104501.

[2] J. Illingsworth, H.M. Ai-Allak, A.W. Brinkman, J. Woods, The influence of Mn on the grain-boundary potential barrier characteristics of donor-doped $BaTi0_3$ ceramics, Journal of Applied Physics 67 (1990) 2088–2092.
[3] W. Heywang, Resistivity anomaly in doped barium titanate, Journal of the American Ceramic Society 47 (1964) 484.
[4] W. Heywang, Barium titanate as a semiconductor with blocking layers, Solid-State Electronics 3 (1961) 51.
[5] G.H. Jonker, Some aspects of semiconducting barium titanate, Solid-State Electronics 7 (1964) 895–903.
[6] P.H. Xiang, H. Harinaka, H. Takeda, T. Nishida, K. Uchiyama, T. Shiosaki, Annealing effects on the characteristics of high T_c lead-free barium titanate-based positive temperature coefficient of resistivity ceramics, Journal of Applied Physics 104 (2008) 094108.
[7] W.H. Yang, Y.P. Pu, X.L. Chen, J.F. Wang, Study of reoxidation in heavily La-doped barium titanate ceramics, Journal of Physics: Conference Series 152 (2009) 012040.
[8] Z.C. Lia, H. Zhang, X.D. Zou, Bill Bergman, Synthesis of Sm-doped $BaTiO_3$ ceramics and characterization of a secondary phase, Materials Science and Engineering, B: Advanced Functional Solid-State Materials 116 (2005) 35.
[9] A. Kanda, S. Tashiro, H. Igarashi, Effect of firing atmosphere on electrical properties of multilayer semiconducting ceramics having positive temperature coefficient of resistivity and Ni-Pd internal electrodes, Japanese Journal of Applied Physics 33 (1994) 5431–5434.
[10] H. Niimi, K. Mihara, Y. Sakabe, M. Kuwabara, Preparation of multilayer semiconducting $BaTiO_3$ ceramics Co-fired with Ni inner electrodes, Japanese Journal of Applied Physics 46 (10A) (2007) 6715–6718.
[11] H. Niimi, Hikone, A. Ando, Omihachiman, Multilayer positive temperature coefficient thermistor and method for designing the same, US Patent 7,348,873 B2 (2008).
[12] Y.K. Chung, S.C. Choi, Effects of the re-oxidation temperature and time on the PTC properties of Sm-doped $BaTiO_3$, Journal of the Korean Chemical Society 46 (2009) 330–335.
[13] J.K. Lee, J.S. Park, K.S. Hong, Role of liquid phase in PTCR characteristics of $(Ba_{0.7}Sr_{0.3})TiO_3$ Ceramics, Journal of the American Ceramic Society 85 (2002) 1173–1179.
[14] H.Y. Chang, K.S. Liu, I.N. Lin, Modification of PTCR behavior of $(Sr_{0.2}Ba_{0.8})TiO_3$ materials by post-heat treatment after microwave sintering, Journal of The European Ceramic Society 16 (1996) 63–70.
[15] M.A. Zubair, C. Leach, Modeling the effect of SiO_2 additions and cooling rate on the electrical behavior of donor-acceptor codoped positive temperature coefficient thermistors, Journal of Applied Physics 103 (2008) 123713.
[16] H.P. Chen, T.Y. Tseng, The effect of cooling rate on the positive temperature coefficient resistivity characteristics of lanthanum-doped $Ba_{0.8}Sr_{0.2}TiO_3$ ceramics, Journal of Materials Science Letters 8 (1989) 1483–1485.
[17] M.A. Zubair, C. Leach, The influence of cooling rate and SiO_2 additions on the grain boundary structure of Mn-doped PTC thermistors, Journal of The European Ceramic Society 28 (2008) 1845–1855.
[18] T.F. Lin, C.T. Hu, Defects restoration during cooling and annealing in PTC type barium titanate ceramics, Journal of Materials Science 25 (1990) 3029–3033.
[19] S.H. Yoon, H. Kim, Space charge segregation during the cooling process and its effect on the grain boundary impedance in Nb-doped $BaTiO_3$, Journal of the European Ceramic Society 22 (2002) 689–696.
[20] J. Qi, Z. Gui, Y. Wang, Q. Zhu, Y. Wu, L. Li, The PTCR effect in $BaTiO_3$ ceramics modified by donor dopant, Ceramics International 28 (2002) 141.
[21] M. Kuwabara, Effect of Microstructure on PTCR in Semiconducting Barium Titanate Ceramics, Journal of the American Ceramic Society 64 (1981) 639–644.
[22] Y.H. Hu, M.P. Harmer, D.M. Smyth, Solubility of BaO in BaTiO3, Journal of the American Ceramic Society 68 (1985) 372.
[23] D.E. Rase, R. Roy, Journal of the American Ceramic Society 38 (1955) 102.
[24] H. Niimi, K. Mihara, Y. Sakabe, Influence of Ba/Ti ratio on the positive temperature coefficient of resistivity characteristics of Ca-doped semiconducting $BaTiO_3$ fired in reducing atmosphere and reoxidized in air, Journal of the American Ceramic Society 90 (6) (2007) 1819.
[25] K. Park, J.G. Kim, K.J. Lee, W.S. Cho, W.S. Hwang, Electrical properties and microstructure of Y-doped $BaTiO_3$ ceramics prepared by high-energy ball-milling, Ceramics International 34 (2008) 1573.
[26] C.J. Johnson, Some dielectric and electro-optic properties of BaTiO3 single crystals, Applied Physics Letters 7 (1965) 221.
[27] B. Huybrechts, K. Ishízaki, M. Takata, Experimental evaluation of the acceptor-states compensation in positive-temperature-coefficient-type barium titanate, Journal of the American Ceramic Society 75 (1992) 722–724.
[28] H.M. AlAllak, J. Illingsworth, A.W. Brinkman, G.J. Russell, J. Woods, The effects of donor dopant concentration on the grain boundary layer characteristics in n-doped $BaTiO_3$ ceramics, Journal of Applied Physics 64 (1988) 6480.
[29] M. Kuwabara, Determination of the potential barrier height in barium titanate ceramics, Solid-State Electronics 27 (1984) 933.